

PROCEEDINGS OF SPIE

[SPIDigitalLibrary.org/conference-proceedings-of-spie](https://spiedigitallibrary.org/conference-proceedings-of-spie)

Time to go $H-\infty$

Toomas Erm, Zdenek Hurak, Bertrand Bauvir

Toomas Erm, Zdenek Hurak, Bertrand Bauvir, "Time to go $H-\infty$,"
Proc. SPIE 5496, Advanced Software, Control, and Communication Systems
for Astronomy, (15 September 2004); doi: 10.1117/12.555606

SPIE.

Event: SPIE Astronomical Telescopes + Instrumentation, 2004, Glasgow,
United Kingdom

Time to go H_∞ ?

Toomas Erm^a, Zdeněk Hurák^b and Bertrand Bauvir^c

^a Astronomy Department., California Institute of Technology, 10524 Caltech, 1201 East California Blvd, Pasadena CA 91125, USA;

^b Center for Applied Cybernetics, Czech Technical University, Karlovo náměstí 13/E, 12135 Prague, Czech Republic;

^c European Southern Observatory, Avda. Balmaceda 2536, Antofagasta, Chile.

ABSTRACT

Traditionally telescope main axes controllers use a cascaded PI structure. We investigate the benefits and limitations of this and question if better performance can be achieved with modern control techniques. Our interest is mainly to improve disturbance rejection since the tracking performance normally is easy to achieve. Comparison is made to more advanced controller structures using H-infinity design. This type of controller is more complex and needs a mathematical model of the telescope dynamics. We discuss how to obtain this model and also how to reduce it to a more manageable size using state of the art model reduction techniques. As a design example the VLT altitude axis is chosen.

Keywords: Very Large Telescope, H-infinity optimal control, cascaded PI, disturbance rejection.

1. INTRODUCTION

Although the tracking of the VLT is excellent and the direct drive main axis servos consistently deliver a position error of less than 10 milliarcseconds the servos are sensitive to disturbances. The altitude axis show more sensitivity to wind disturbance than the azimuth. Image degradation due to wind disturbance is effectively reduced by the M2 field stabilization. Yet, there are circumstances where better disturbance rejection is desirable without relying on field stabilization. The axis servo can be represented as shown in Fig. 1.

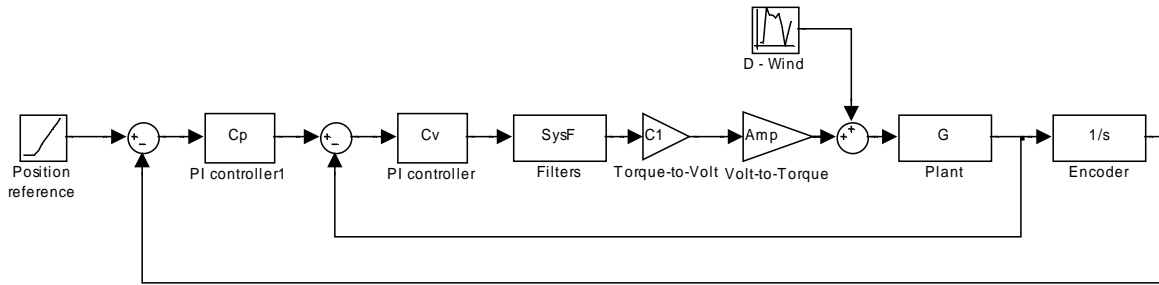


Figure 1. Block diagram of the existing control system

The block diagram allows us to create a transfer function from torque to position that we call the disturbance transfer function (DTF). The scale factors C1 and Amp are used to illustrate how the DTF was measured.

$$DTF(s) = \frac{G \cdot \frac{1}{s}}{(1 + Amp \cdot G \cdot (C_p \cdot \frac{1}{s} + 1) \cdot C_v \cdot SysF \cdot C_1)} \quad (1)$$

The units are conveniently arranged as rad/Nm and describe the position error resulting from a disturbance in the torque. DTF have been measured for all UT's and optimized accordingly. The limitations of the cascaded PI controllers

prevent us from further improvement of the DTF and therefore new methods found in modern control theory have been explored. As a reference for further improvement the optimal DTF achieved with the cascaded PI control has been used. An improvement of a factor 2 in DTF is the goal of the investigation; a factor 4 would be desirable and constitute a significant improvement.

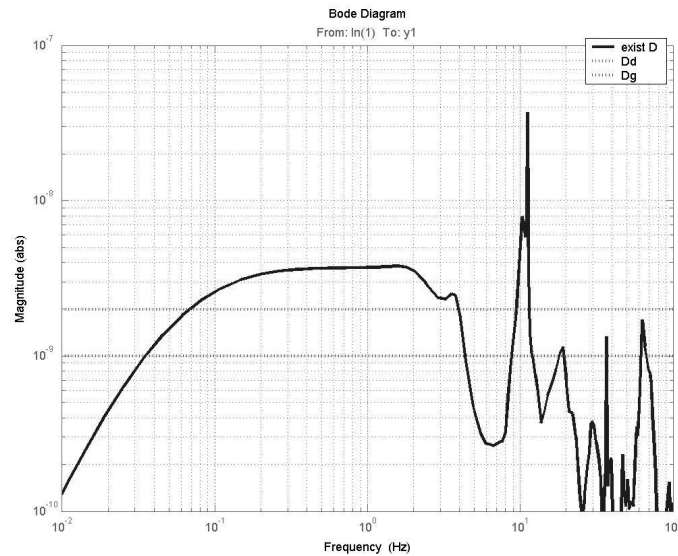


Figure 2. DTF for existing system

To avoid misunderstandings it must be pointed out that the DTF measures only errors in the axis position error due to torque disturbances and is only a part of the total image jitter. Fig. 2 shows the DTF for the existing controller with the two design goals superimposed.

2. WIND DISTURBANCE

Wind tunnel tests have been performed at The Danish Maritime Institute within the frame of the VLT project and resulted in a wind disturbance model shown in Fig. 3.

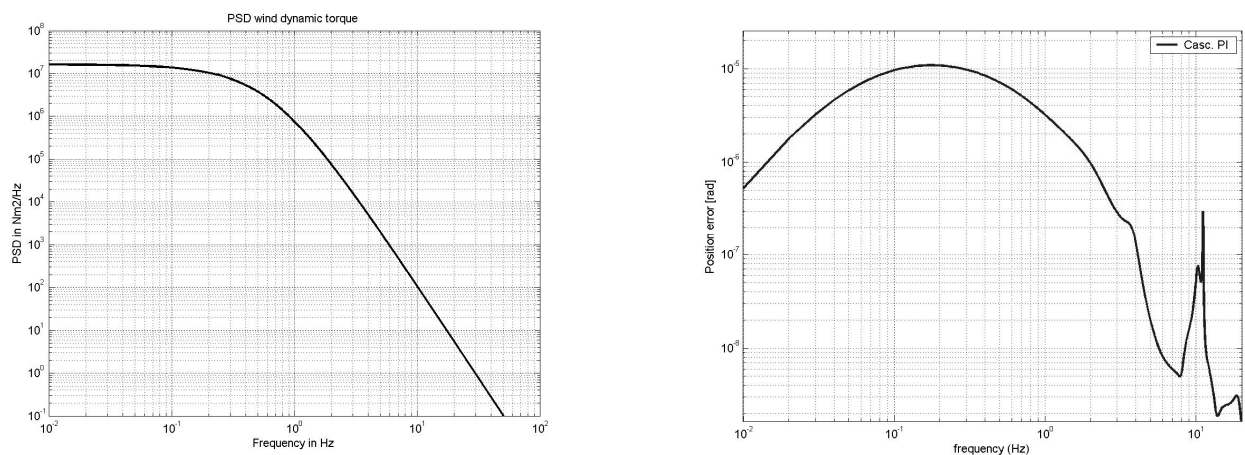


Figure 3. Modeled wind torque and the resulting position error with the actual controller configuration

3. LUMPED LINEAR MODEL FROM SYSTEM IDENTIFICATION

A mathematical model was sought for a system with only one input - a control voltage [V] - and one measured output - the angular velocity [rad/s]. A lumped linear model of order 60 has been obtained from an experimental system identification procedure. The data was measured with sampling period 5 ms. The controller design is performed in continuous time domain and therefore it must be kept in mind that the corresponding continuous time models are only valid up to 100 Hz ($\cong 600$ rad/s).

4. MODEL ORDER REDUCTION

Numerical solvers for control synthesis might have troubles with high order models. It is therefore necessary to find a lower order approximated model for the plant while preserving important characteristics of the original model. A crucial step is to determine the order of the approximate model. Guidance is provided by Hankel singular values of the system which are visualized in Fig. 4. A common method of model order reduction is used that relies on transformation of a state space model to a balanced realization, and deletion of several least significant state variables¹.

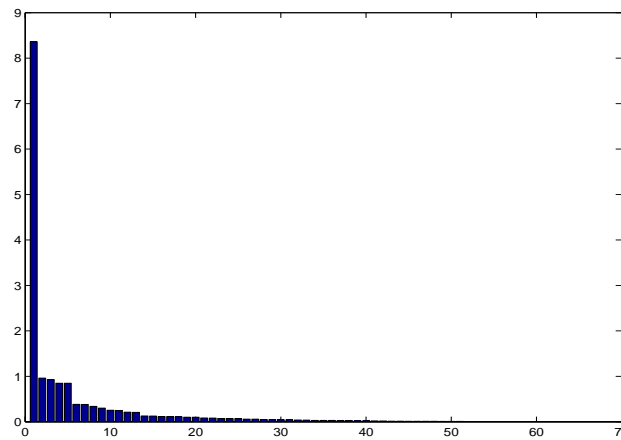


Figure 4. Hankel singular values for the full order model produced by Matlab balreal function

The two computational steps are implemented in functions balreal and modred in Matlab. A comparison of magnitude frequency responses of the full order lumped linear model and the reduced model of order 24 is given in Fig. 5. Note that, for angular position control, the reduced model dynamics must be augmented by an integrator.

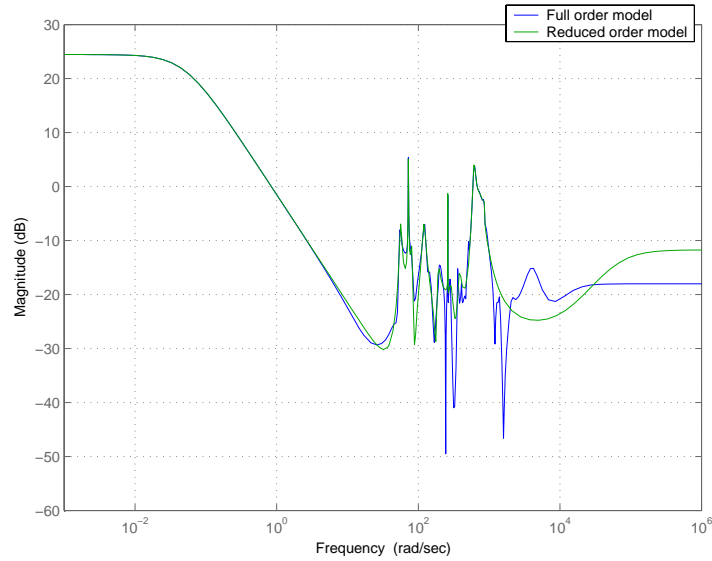


Figure 5. Frequency response of the full and reduced order models with angular rate as an output

5. ACHIEVABLE BANDWIDTH

One of the ambitions of a controller design via minimization of the H-infinity norm of a mixture of sensitivity functions is to extend the bandwidth as high as possible and then roll off (decrease in magnitude) very fast respecting the weakly damped structural modes. The rationale is that the higher the closed loop bandwidth, the better the attenuation of effects of disturbing wind buffeting. Unfortunately, the highest achievable bandwidth is constrained by some inherent limitations. One of them is expressed by the so called area formula; see Ref. 1 or Ref. 2 for detailed explanations. Assuming the least constrained case when both the plant and the controller are strictly proper and stable, this formula goes

$$\int_0^{\infty} \ln|S(j\omega)| d\omega = 0 \quad (2)$$

where $S(s)$ is a sensitivity function. Loosely speaking, the frequency regions where logarithm of a magnitude frequency response is negative, which is desirable, must be compensated for by regions with positive $\ln|S(j\omega)|$, which is undesirable. At first, this does not seem to be a significant constraint, as the whole frequency axis is available for making up for the negative regions in the integral. Yet, this is not true in practical applications³. The formula (2) is of theoretical value only. In real applications like the control of a telescope, the true available bandwidth is limited by the frequency of the first lightly damped structural modes, which is about 8 Hz (50 rad/s) for the altitude axis of the VLT. Above that frequency, the credibility of the model decreases significantly. The area formula is then changed to a more realistic form

$$\int_0^{2\pi \cdot 8} \ln|S(j\omega)| d\omega = 0 + \text{some small term} \quad (3)$$

Most control applications share the design requirements: attenuation of disturbances at low frequencies, a peak in magnitude of the frequency response no higher than something like 1.5 dB, complete attenuation of constant disturbances (type I control). These requirements can be expressed using a template as Fig. 6.

Expressing the function $\ln|S|$ as a function of frequency and of parameters f_1 , f_2 , f_3 and m and substituting it into (3), the minimum achievable peak in the sensitivity function as a function of a parameter f_b goes

$$\sigma = e^{\frac{f_1 \ln(2\pi m) - f_1 + (f_2 - f_1) \ln m}{f_2 - f_3}} \quad (4)$$

The crucial parameter is the bandwidth f_2 . A dependence of σ on it is visualized at Fig. 6 for the remaining parameters set to reasonable values ($f_1 = 0.01\text{Hz}$, $f_3 = 8\text{Hz}$ and $m = 0.01$).

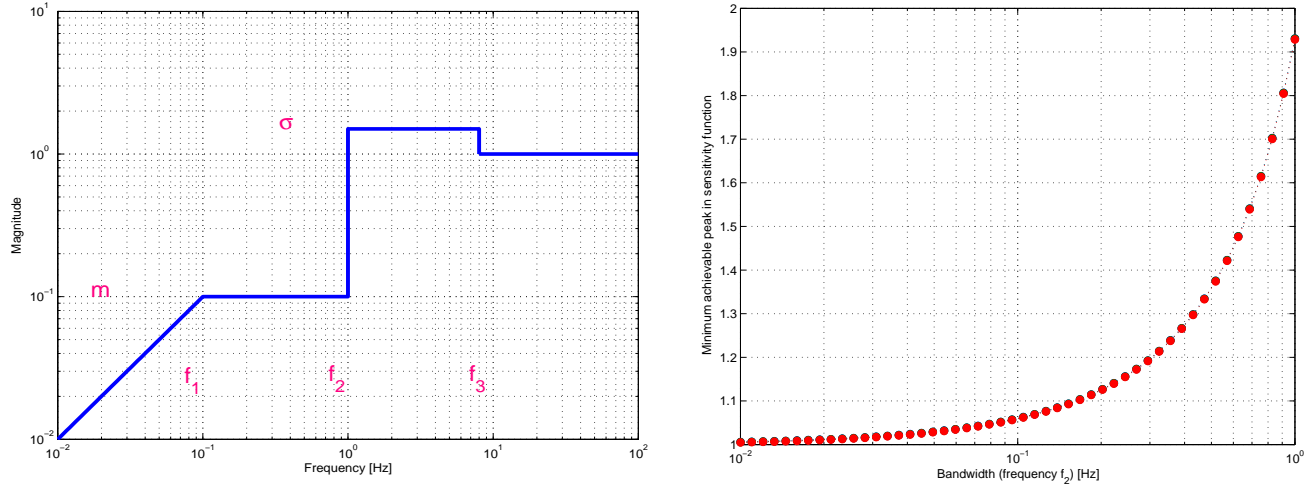


Figure 6. Template for a sensitivity function $\ln |S|$ for an acceptable design and minimum achievable peak for a logarithm of a sensitivity function as a function of a bandwidth (parameter f_2). The other parameters for the template set to $f_1 = 0.01\text{Hz}$, $f_3 = 8\text{Hz}$ and $m = 0.01$.

6. MIXED SENSITIVITY MINIMIZATION

6.1 Standard mixed sensitivity problem

Given a lumped linear time-invariant model of the system that relates the control voltage applied to the armature of the motor and the angular position that can be described either using a transfer function $G(s) = b(s)/a(s)$ or using a state-space model representation

$$\begin{aligned} \dot{x}_G(t) &= A_G x_G(t) + B_G u_G(t) \\ y_G(t) &= C_G x_G(t) + D_G u_G(t) \end{aligned} \quad (5)$$

The objective of the control synthesis is to find a stabilizing feedback controller with a transfer function $C(s)$ that minimizes the $\sup_{\omega} \|W1(i\omega)S(i\omega)\| + \|W3(i\omega)T(i\omega)\|$, where $S(s) = 1/(1 + G(s)C(s))$ and $T(s) = G(s)C(s)/(1 + G(s)C(s))$ are the sensitivity and complementary sensitivity functions respectively, and $W1(s)$ and $W3(s)$ are the design specifications that take the form of weighting filters. Combining both sensitivity functions into one optimization criterion guarantees good performance and robustness against uncertainties in the model, especially at higher frequencies². These uncertainties are induced here by the reduction of the order of the model. The standard configuration for a mixed sensitivity minimization based design is shown in Fig. 7. The actual computational tool used to solve this standard problem is the `hinftopt` function of Matlab Robust Control Toolbox⁴ that implements Safonov's improved loop-shifting "two-Riccati-equation" method⁵.

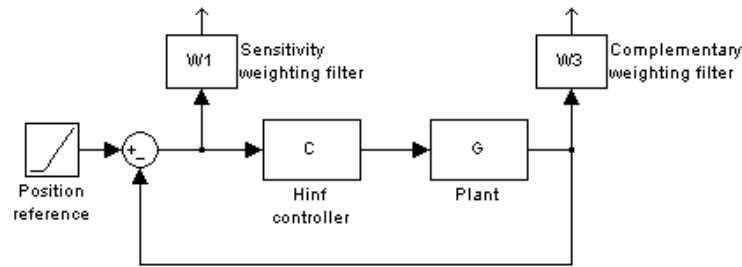


Figure 7. Standard feedback configuration for a mixed sensitivity minimization controller design

The $W1(s)$ weighting filter penalizes the control error. By choosing a low-pass characteristic for this specification criterion, the resulting controller is such that the error signal is small for low frequencies. The $W3(s)$ weighting filter determines the attenuation at higher frequencies; i.e. its inverse describes asymptotically the closed loop transfer function. It is usually sufficient to choose a simple form for it, like $W3(s)=s^2/k_3$. The complementary sensitivity function will be shaped by the inverse of $W3(s)$ filter; i.e. it will roll off at 40 dB per decade.

6.2 Disturbance rejection

The previous design scheme focuses on shaping the sensitivity and complementary sensitivity functions. The minimization of complementary sensitivity function $T(s)$ at higher frequencies expresses the robustness requirements, while the sensitivity function $S(s)$ expresses the requirements on tracking performance and also disturbance rejection with the disturbing variable corrupting the output from the plant. Since the disturbance considered here is a torque induced by the wind affecting the whole system, it is naturally modeled as a signal corrupting the input to the plant.

The objective is to specify a design criterion to shape the disturbance sensitivity function. It is accomplished by introducing a new exogenous signal that affects the plant at its input and filtering it through a disturbance weighting function $W4(s)$ that usually takes the form of a low pass filter⁶.

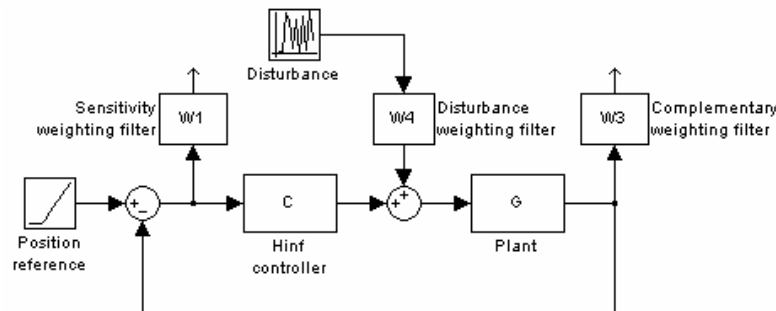


Figure 8. Feedback configuration for the general H-infinity control problem with disturbance rejection capability

Matlab Robust Control Toolbox does not offer a convenient way for creating a generalized plant including a disturbance weighting filter. Yet, deriving a state-space model for it is quite straightforward after re-structuring the plant, augmented with the weighting filters, into the system shown in Fig. 9.

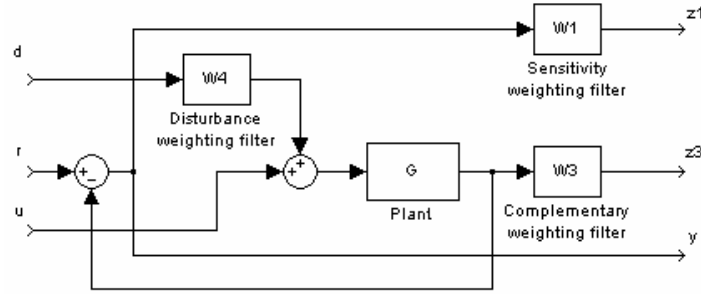


Figure 9. General H-infinity augmented plant

$$\begin{bmatrix} \dot{x}_G(t) \\ x_1(t) \\ x_3(t) \\ x_4(t) \end{bmatrix} = \begin{bmatrix} A_G & 0 & 0 & B_G C_4 \\ -B_1 C_G & A_1 & 0 & -B_1 D_G C_4 \\ B_3 C_G & 0 & A_3 & B_3 D_G C_4 \\ 0 & 0 & 0 & A_4 \end{bmatrix} \begin{bmatrix} x_G(t) \\ x_1(t) \\ x_3(t) \\ x_4(t) \end{bmatrix} + \begin{bmatrix} 0 & B_G D_4 & B_G \\ B_1 & -B_1 D_G D_4 & -B_1 D_G \\ 0 & B_3 D_G D_4 & B_3 D_G \\ 0 & B_4 & 0 \end{bmatrix} \begin{bmatrix} r(t) \\ d(t) \\ u(t) \end{bmatrix} \quad (6)$$

$$\begin{bmatrix} z_1(t) \\ z_3(t) \\ y(t) \end{bmatrix} = \begin{bmatrix} -D_1 C_G & C_1 & 0 & -D_1 D_G C_4 \\ D_3 C_G & 0 & C_3 & D_3 D_G C_4 \\ -C_G & 0 & 0 & -D_G C_4 \end{bmatrix} \begin{bmatrix} x_G(t) \\ x_1(t) \\ x_3(t) \\ x_4(t) \end{bmatrix} + \begin{bmatrix} D_{11} & -D_1 D_G D_4 & -D_1 D_G \\ 0 & D_3 D_G D_4 & D_3 D_G \\ 1 & -D_G D_4 & -D_G \end{bmatrix} \begin{bmatrix} r(t) \\ d(t) \\ u(t) \end{bmatrix}$$

If the $W3(s)$ weighting filter is non proper, it has no state space representation. In the case of the $W3(s)$ filter form proposed in the previous section and assuming that the interconnected system is proper, the state-space representation of the augmented system becomes

$$\begin{bmatrix} \dot{x}_G(t) \\ x_1(t) \\ x_4(t) \end{bmatrix} = \begin{bmatrix} A_G & 0 & B_G C_4 \\ -B_1 C_G & A_1 & -B_1 D_G C_4 \\ 0 & 0 & A_4 \end{bmatrix} \begin{bmatrix} x_G(t) \\ x_1(t) \\ x_4(t) \end{bmatrix} + \begin{bmatrix} 0 & B_G D_4 & B_G \\ B_1 & -B_1 D_G D_4 & -B_1 D_G \\ 0 & B_4 & 0 \end{bmatrix} \begin{bmatrix} r(t) \\ d(t) \\ u(t) \end{bmatrix} \quad (7)$$

$$\begin{bmatrix} z_1(t) \\ z_3(t) \\ y(t) \end{bmatrix} = \begin{bmatrix} -D_1 C_G & C_1 & -D_1 D_G C_4 \\ C_{21} & 0 & C_{23} \\ -C_G & 0 & -D_G C_4 \end{bmatrix} \begin{bmatrix} x_G(t) \\ x_1(t) \\ x_4(t) \end{bmatrix} + \begin{bmatrix} D_{11} & -D_1 D_G D_4 & -D_1 D_G \\ 0 & D_{22} & D_{23} \\ 1 & -D_G D_4 & -D_G \end{bmatrix} \begin{bmatrix} r(t) \\ d(t) \\ u(t) \end{bmatrix}$$

where

$$\begin{aligned} C_{21} &= C_G A_G^2 / k_3 \\ C_{23} &= (C_G A_G B_G C_4 + C_G B_G C_4 A_4 + D_G C_4 A_4^2) / k_3 \\ D_{22} &= (C_G A_G B_G D_4 + C_G B_G C_4 D_4 + D_G C_4 A_4 B_4) / k_3 \\ D_{23} &= C_G A_G B_G / k_3 \end{aligned} \quad (8)$$

7. A TWO DEGREES-OF-FREEDOM H-INFINITY CONTROLLER

Recognizing that the closed loop bandwidth really didn't need any improvement (the tracking performance of the VLT main axes is 10 times better than the original specifications) lead to the idea of a two degrees-of-freedom (2DOF)

controller; i.e. the controller is separated into a disturbance controller and a tracking controller which can be optimized independently.

Here, the H-infinity optimization criteria focus on disturbance rejection, neglecting tracking capabilities of the closed loop system. Once a suitable setting is found, the resulting controller can be moved to the feedback path of the loop. The tracking control is achieved by placing in the reference path a pre-filter optimized to arbitrarily shape the closed loop response as it has no influence on the stability of the loop.

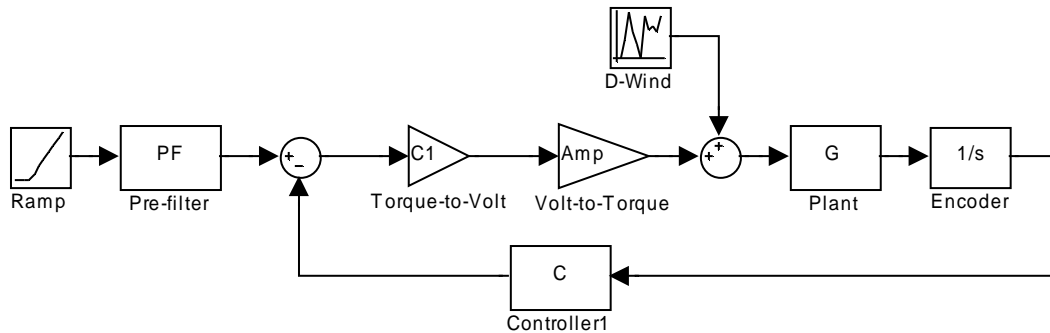


Figure 10. H-infinity based two degrees-of-freedom controller

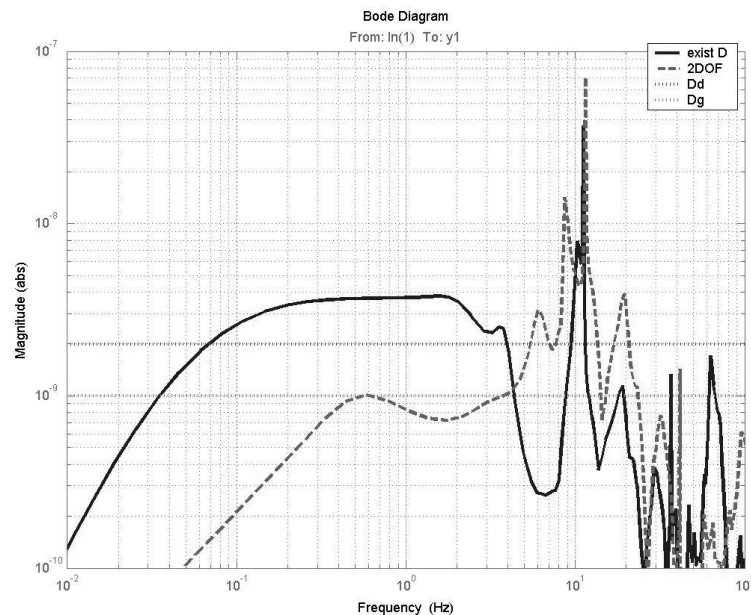


Figure 11. Comparison of DTF of the actual cascaded PI and the 2DOF controllers. A 12 dB improvement is achieved.

8. H-INFINITY VELOCITY CONTROLLER

The second controller design investigated consists of a H-infinity based velocity loop combined with a standard position loop. This combination seems to be far superior to the existing solution and comparable to the H-infinity based two degrees-of-freedom controller.

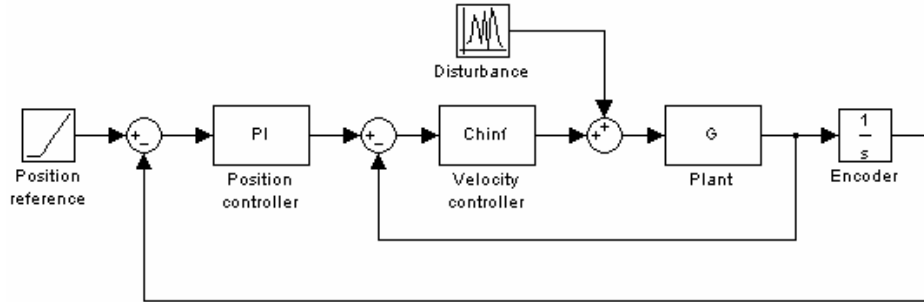


Figure 12. Velocity loop replaced with H-infinity controller

The optimal controller configuration was found with

$$\begin{aligned}
 W_1(s) &= 30 / (0.01s^2 + 0.2s + 1) \\
 W_3(s) &= 0.02s \\
 W_4(s) &= 30 / (0.1s + 1) \\
 PI(s) &= (8.5s + 2) / s
 \end{aligned}
 \tag{9}$$

This solution has the advantage of minimal implementation efforts. In most telescopes using a velocity loop implemented with analog electronics it's simply a matter of replacing it with a small amount of new software. The position loop will still handle all the overhead with limit checking, trajectory generation, etc.

Fig. 13 shows the DTF of the three controller structures considered here. Both H-infinity based controllers offer better disturbance rejection than the cascaded PI.

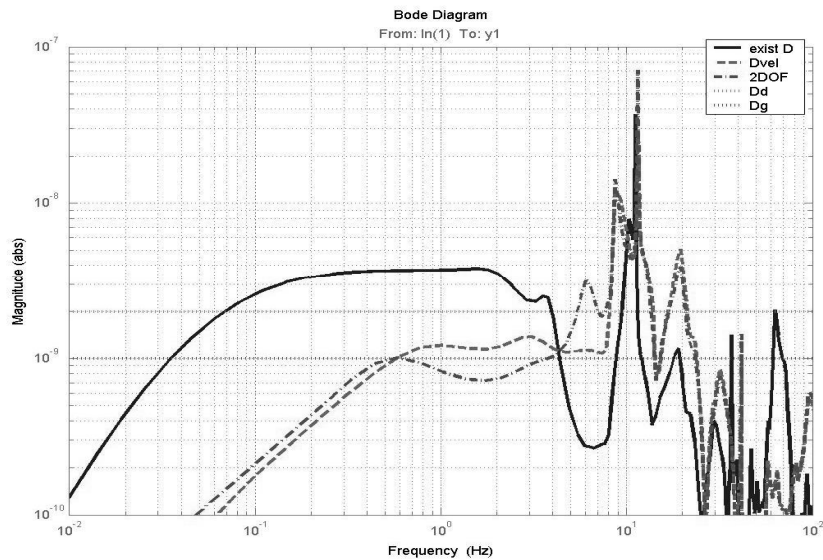


Figure 13. Comparison of the DTF of the 3 different systems

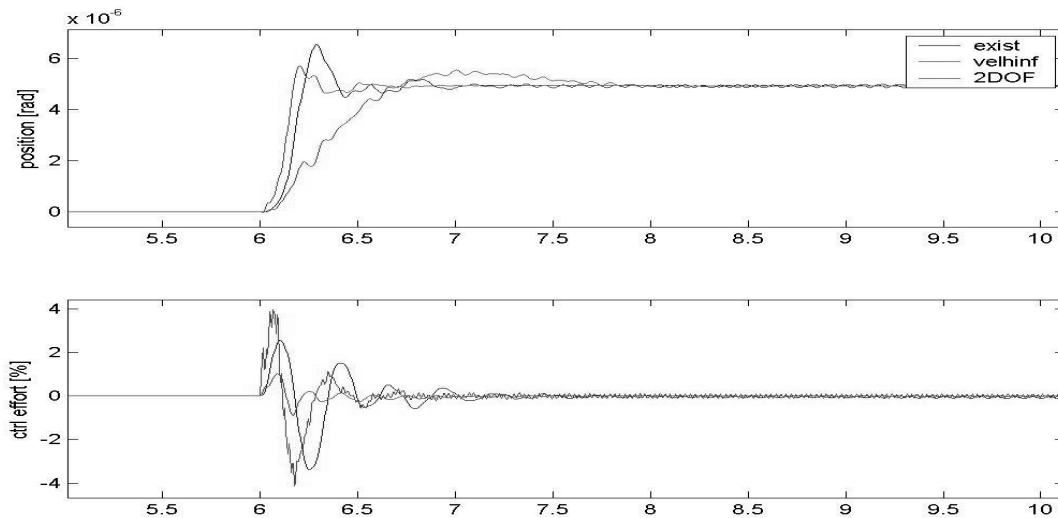


Figure 14. Closed loop response and control effort for a 1 arcsecond step

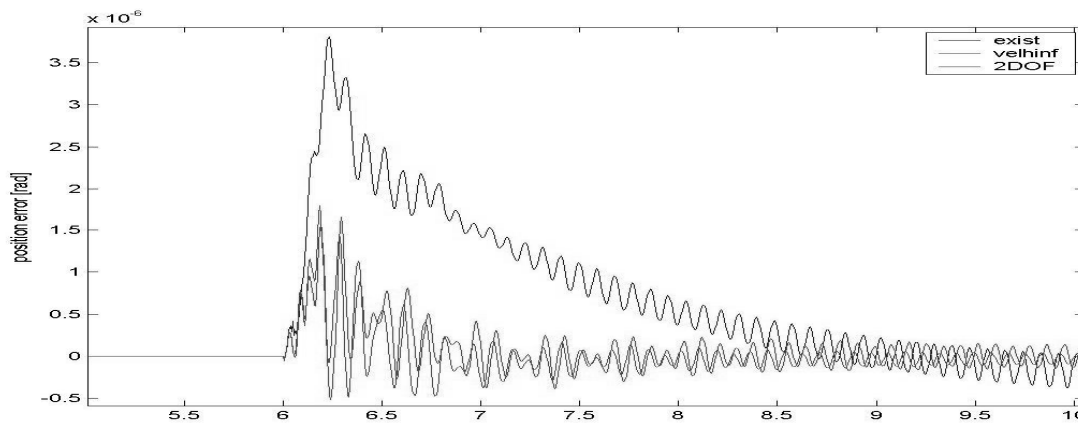


Figure 15. Position errors resulting from a 1000 Nm step disturbance

9. CONCLUSIONS

An outline of a controller design procedure for elevation axis positioning of a VLT telescope was given in this paper. The existing control system based on two cascaded PI loops with structural filters was contrasted to controllers designed using advanced minimization of H-infinity norm of mixed sensitivity function. The objective of this report is to share the experience gained using these advanced control design methods and to estimate if this new control design paradigm is really to replace the cascaded PI approach used by generations of engineers. The standard mixed sensitivity minimization that features two weighting filters $W1(s)$ and $W3(s)$ is a very elegant design procedure with intuitive interpretation of the design criteria into parameters of the two weighting filters. It does not however, capture the major design objective, i.e. the attenuation of disturbing torque induced by wind buffeting. To take this disturbance into consideration in controller design, the generalized plant must be augmented by another input weighted by a filter $W4(s)$. This seems a natural step but the conflicting interest of tracking performance and disturbance rejection are not easily satisfied with the standard H-infinity approach and special configuration like hybrid controllers have to be used. This

was shown by replacing the velocity PI controller in a standard cascaded loops system with a H-infinity based controller and a two degrees-of-freedom H-infinity controller. Both satisfy the design goals and improve the disturbance rejection by 12 dB. It was the intention to have real test result of the VLT altitude axis presented in this paper but time constraints and other commitment of the authors made it impossible. We are expecting to be able to perform the test within the near future.

To answer the question in the title of this paper, we definitely think that “going H-infinity” is a solution to improvement of the wind rejection for most telescopes.

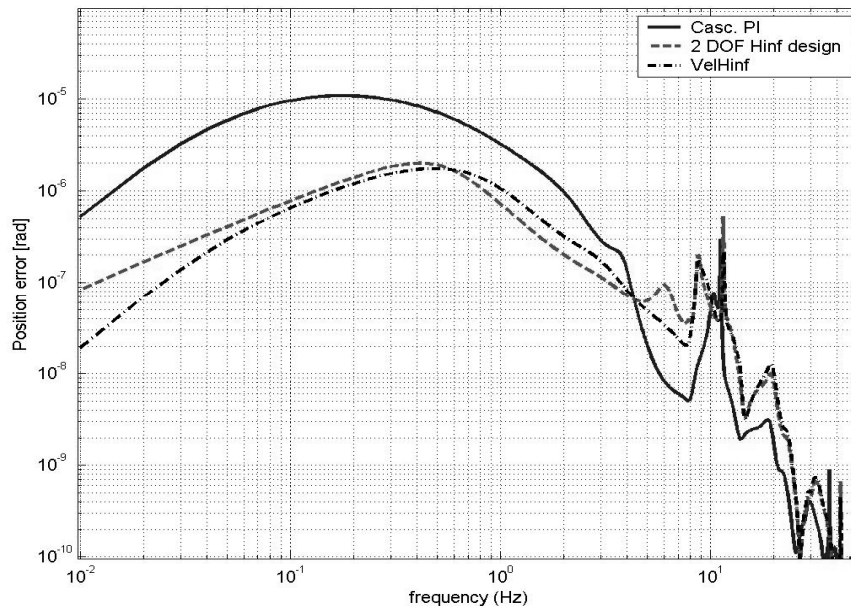


Figure 16. The 3 systems exposed to the same wind load

ACKNOWLEDGMENTS

This research work was supported by the European Southern Observatory (ESO) and Ministry of Education of the Czech Republic under Project LN00B096.

REFERENCES

1. K. Zhou, J. C. Doyle, and K. Glover, *Robust and optimal control*, PrenticeHall Inc., Upper Saddle River, NJ 07458, 1996.
2. J. Doyle, B. Francis, and A. Tannenbaum, *Feedback Control*, Macmillan Publishing Co., New York, 1990.
3. G. Stein, “Respect the unstable”, *IEEE Control Systems Magazine* 23, pp. 12--25, 2003.
4. The Mathworks Inc., *Robust Control Toolbox for Use with Matlab, 2nd ed.*, 2001.
5. M. G. Safonov, D. J. N. Limebeer, and R. Y. Chiang, “Simplifying the H-infinity theory via loop shifting, matrix pencil and descriptor concepts”, *International Journal of Control* 50(6), pp. 2467--2488, 1989.
6. Gustavo A. Medrano Cerda et al., “H-Infinity motion control system for a 2 m telescope”, *SPIE*, 2002.
7. Marco Quattri, Franz Koch, “Enclosure and infrastructure requirements for OWL: possible solutions”, *Proc. SPIE* Vol. 4004, p. 509-516, 2000.
8. W. Gawronski, JPL, “A H-infinity controller with wind disturbance rejection properties for the DSS-13 Antenna”, *TDA progress report 42-127*, 1996.